Design Investigation of a Wideband Backward-Wave Directional Coupler Using Neural Network

Zahra S. Tabatabaeian
Electrical Department,
Ferdowsi University of Mashhad,
Mashhad, Iran.
ztaba14@gmail.com

Mohammad H. Neshati
Electrical Department,
Ferdowsi University of Mashhad,
Mashhad, Iran.
neshat@um.ac.ir

***Abstract*— The current paper presents a study of wideband backward-wave directional coupler. In designing this coupler, neural network technique has been employed. This coupler has high coupling in a wide bandwidth. Composite right left handed (CRLH) behavior of defected ground structure (DGS) and connections between coupled lines cause these characteristics. This coupler is fabricated. Fabrication results agree well with simulation results.**

Keywords: *directional coupler, neural network, composite right left handed (CRLH), defected ground structure (DGS).*

I. INTRODUCTION

Directional couplers are generally used in microwave and millimeter wave circuits, such as filter, balun [1], transformer and power divider [2]. The coupling mechanism in these devices is including two kinds [3], which depend on the structure of the coupled line and the interspacing between them. The first mechanism is the backward coupler, in which coupling mechanism is based on the difference between the even- and odd-mode characteristic impedance of the lines. To increase the difference between characteristic impedances, the distance between the lines may be reduced. However, this is difficult because of the fabrication constrains and therefore, low coupling level is the most important limitation of the backward couplers. The second mechanism in couplers is based on the difference between phase velocities of even- and odd-modes leading to realization of forward couplers. Unlike backward couplers, coupling in forward couplers could be as high as 0 dB.

Nevertheless, implementing these components by planar microstrip coupled lines has two drawbacks. The first one is the small difference between even- and odd-mode propagation constants, which requires very long coupling length. The second drawback is non-identical characteristic impedances of even- and odd-modes, which degrade the coupling level, which, in turn decrease directivity performance of the coupler.

Lange coupler is a planar coupler that is widely used in practical communication systems. It provides both broad bandwidth and tight coupling [4]. This coupler also suffers from a drawback, which requires bulky bonding wires leading to parasitic effects at high frequencies.

In recent years, composite right left-handed (CRLH) couplers have been utilized as unique alternatives to the Lange coupler [5]. These couplers offer tight coupling over a broad bandwidth due to their planar structure, bonding wires is not required. In CRLH couplers, even- and odd-mode characteristic impedances are purely imaginary in their coupling bandwidth. Therefore, coupling level is not related to the electrical length of the lines. Instead, it depends on the attenuation length of the modes.

In the present study, a low profile wideband backward-wave directional coupler is designed and optimized using neural network. The coupler provides similar performances to that of CRLH couplers over a wide bandwidth. To obtain this behavior, two mechanisms have been employed. First, series capacitance is added for even mode using Defected Ground Structure (DGS) patterns. The second utilized technique is connections between the coupled lines, which provide shunt inductance for odd modes. One prototype of the proposed coupler is made and a few characteristics of the coupler are measured. Also a full wave analysis using High Frequency Structure Simulator (HFSS) is applied and coupler performances are numerically investigate the proposed.

II. COUPLER STRUCTURE

Fig. 1 shows the proposed structure of the directional coupler. l and h denote length and thickness of the substrate respectively. W is the coupled line width and they are separated from each other by s. This coupler is symmetric along AA' line and the connections between the lines are the same. The Defected Ground Structure (DGS) slots are etched at the bottom layer of the substrate and they are separated by t.

As this four port coupler is symmetric, it can be decomposed to even-mode and odd-mode two port structures. Fig. 2a and 2b show the equivalent circuit models for even-

and odd-modes respectively. The propagation of odd-mode has low returned current density on the ground plane for the microstrip coupled line and current goes from one of the coupled lines and returns from the other one. But, the propagation of even-mode has high returned current density on the ground plane of the structure. This is due to the direction of the current of even-mode on the two lines is the same and the return current is directed by ground. Therefore, only the current pattern on the ground plane is affected by the even-mode equivalent circuit. Furthermore, even- and odd-mode equivalent circuit models correspond to the structure with perfect electric wall and perfect magnetic wall at the center of the coupler, respectively.

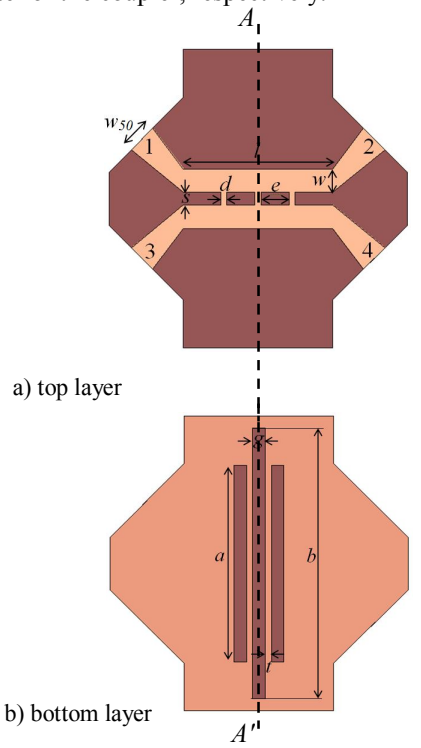

Fig. 1: The structure of the proposed coupler

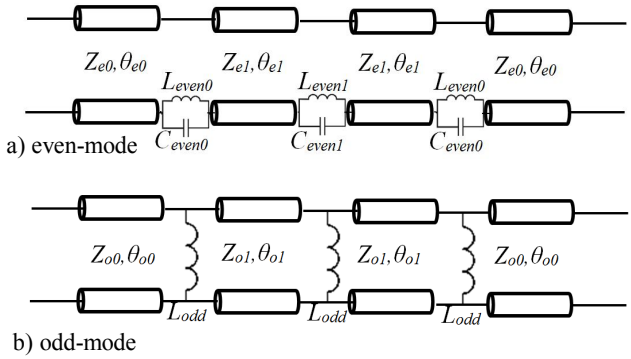

Fig. 2: The equivalent circuit for even- and odd-modes of the proposed coupler

Resonating parallel *LC* circuit for even-mode is used to model the DGS patterns in this coupler. Inductances for odd-mode and capacitances for even-mode model connections between coupled lines. However, the short length of these connections may lead to neglecting the equivalent capacitances for even-mode.

III. Design Procedure

Back propagation neural network (BPNN) is used for designing the proposed coupler. Research has shown that any continuous function in enclosed interval can be approached by a BPNN with a hidden layer. The network that has been shown in Fig. 3 has been employed in this study. In this network, 7 dimensions of the coupler are considered as the inputs, and coupling bandwidth with 1 dB flatness, S_{11} maximum in pass band and S_{41} maximum in pass band are considered to be the outputs of the neural network. 14 neurons exist in the hidden layer [6].

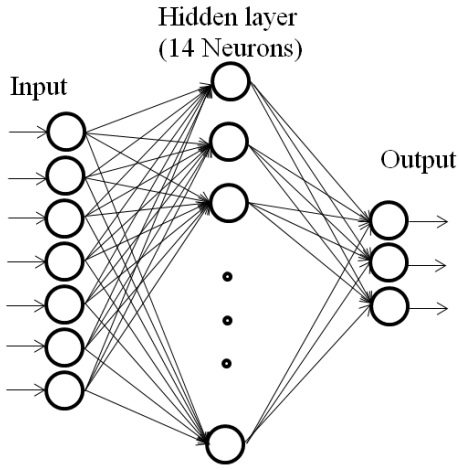

Fig. 3: Back propagation neural network model

These networks have to be trained. Input vectors and the corresponding target vectors are utilized to train the network. BPNN use a gradient descent algorithm in which the network weights are moved along the negative of the gradient of the performance function. The trainbr training function is chosen to train the network in this paper. Based on Levenberg-Marquardt optimization process, training function updates the weight and bias values. To provide a network that generalizes well, it minimizes a combination of squared errors and weights, and then determines the correct combination [7].

For training, the following dimensions are chosen to be the input of the network and coupling bandwidth with 1 dB flatness, S_{11} maximum and S_{41} maximum are tend to be outputs. *b* is chosen from 18 mm to 22 mm, *g* is varied from 0.5 mm to 1.5 mm, *a* is selected from 14 mm to 18 mm, *s* from 0.5 mm to 1.5 mm, *d* from 0.25 mm to 1.25 mm, *e* from 1 mm to 2.5 mm and *w* from 1.6 mm to 2.4 mm. These dimensions are chosen to be the input of the network. Table 1 shows few training data and *T* is defined by equation (1).

$$T = \frac{BW}{MS_{11}MS_{41}} \tag{1}$$

In (1), BW, MS_{11} and MS_{41} are coupling bandwidth with 1 dB flatness, maximum of S_{11} in pass band and maximum of S_{41} in pass band, respectively. Large values of T show better performance for the coupler. BW, MS_{11} and MS_{41} in equation (1) are obtained using HFSS.

If the BPNN is properly trained, it is likely to give reasonable answers when presented with inputs that it has never seen. Testing data are shown in Table II, which show that the BPNN outputs agree well with those obtained by HFSS.

After training the network, optimum values of the inputs in which T is maximum can be obtained. Table 3 summarizes the values for the optimum parameters of the coupler.

Table I: Training data for design procedure.

g	*a*	*b*	*s*	*e*	*d*	*W*	*T*
0.5	14	18	1	2	1	2	107
0.75	16	18	0.5	1	0.75	1.8	143
1	14	18	0.75	1.5	0.5	2.2	166
1.25	18	20	1.25	1.75	0.25	1.6	82
1.5	18	22	1.5	1.25	1.25	2.4	93
0.75	14	20	1	2.25	0.5	1.6	59
1	16	22	0.75	1	1	2	98

g, a, b, s, e, d and *W* in mm.

Table II. Testing data for design procedure

g	*a*	*b*	*s*	*e*	*d*	*W*	*T* BPNN	*T* HFSS
1.2	15	19	0.9	2.4	0.4	1.9	161	155
0.7	17	21	1.3	1.1	0.8	1.7	110	109
1.1	16	20	0.6	1.4	0.7	2.3	89	98
0.8	18	22	1	1.7	0.35	2.1	147	140
1.4	14	18	1.5	1.9	1.1	1.8	96	101
0.7	16	19	0.5	2.4	1	2	29	32
0.8	17	20	1.4	1.5	0.4	2.1	133	128

g, a, b, s, e, d and *W* in mm.

Table III. Optimum values of the proposed coupler parameters.

Parameter	Value (mm)	Parameter	Value (mm)
g	1	*d*	0.5
a	16	*W*	1.9
b	22	*l*	12
s	1	*h*	0.787

IV. Numerical Results and Discussion

Fig. 4 depicts simulated *S*-parameters of the designed coupler versus frequency using the optimized parameters. As this figure shows, the coupler provides 0.58 dB coupling with 1 dB flatness from 6.5 GHz to 14 GHz. This corresponds to 73.2% fractional bandwidth. Reflection coefficient in pass band for the proposed coupler is less than -10 dB over the mentioned bandwidth. Also, directivity in this band is at least 13.83 dB. Considering these results, the derived T value is 180.3 which is very high and agrees well with that obtained by BPNN, which is 188.7. The designed coupler is only $0.56\lambda_g$ long.

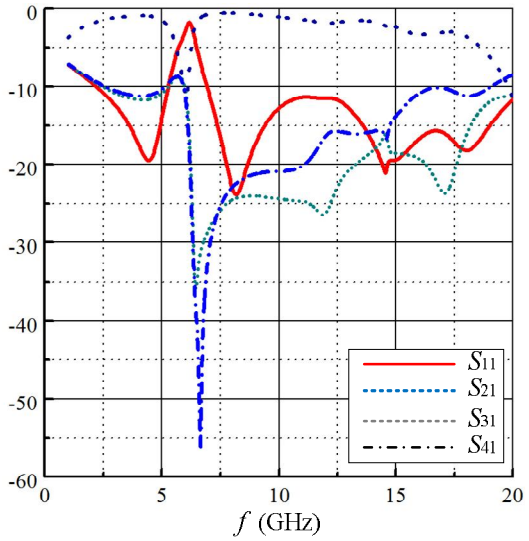

Fig. 4: Simulated *S*-parameters of the proposed coupler.

By calculating even- and odd-mode complex propagation constants and characteristic impedances of these modes, one can understand the cause of high coupling in wide bandwidth. For this, equations (2) and (3) are used respectively.

$$e^{\gamma_i d} = \frac{1 - S_{11,i}^{\ 2} + S_{21,i}^{\ 2} + \sqrt{\left(1 + S_{11,i}^{\ 2} - S_{21,i}^{\ 2}\right)^2 - \left(2S_{11,i}\right)^2}}{2S_{21,i}} \qquad (2)$$

$$\gamma_i = \alpha_i + j\beta_i$$

$$Z_i = Z_0 \sqrt{\frac{\left(S_{21,i}^{\ 2} - S_{11,i}^{\ 2} - 1\right) - 2S_{11,i}}{\left(S_{21,i}^{\ 2} - S_{11,i}^{\ 2} - 1\right) + 2S_{11,i}}} \qquad (3)$$

In the above equations, i represents even- or odd-modes and Z_0 stands for port impedances which is normally 50 Ω. Furthermore, coupling in a backward coupler can be derived by eq. (4).

$$C_z = S_{31} = \frac{(Z_e - Z_o)\tanh(\alpha + j\beta)l}{2Z_0 + (Z_e + Z_o)\tanh(\alpha + j\beta)l} \qquad (4)$$

Fig. 5 demonstrates the variation of $\tanh(\alpha + j\beta)l$ versus frequency. It can be seen that in pass band this function is equal to 1, except from 10 GHz to 13 GHz. So, coupling in this bandwidth can be obtained using the equation (5).

$$C_z = S_{31} = \frac{Z_e - Z_o}{2Z_0 + (Z_e - Z_o)} \quad (5)$$

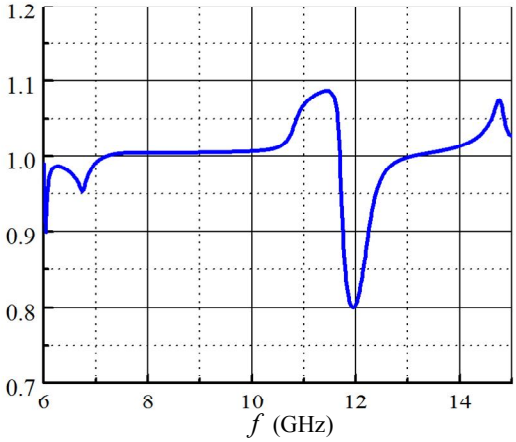

Fig. 5: Variation of $\tanh(\alpha + j\beta)l$ versus frequency.

Fig. 6 presents imaginary part and real part of even and odd-mode impedances, Z_e and $Z_{o,}$. This figure shows that real parts of impedances are negligible in pass band, except from 10 GHz to 13 GHz. It also shows that the imaginary parts in this band have opposite signs. So, coupling C_z is obtained 0 dB in this frequency band.

In frequency range from 10 GHz to 13 GHz $\tanh(\alpha + j\beta)l$ is not equal to 1. However, in this band, imaginary and real parts of Z_e are much greater than imaginary and real parts of Z_o respectively. Therefore, the coupling, C_z, is equal to 0 dB in this frequency range.

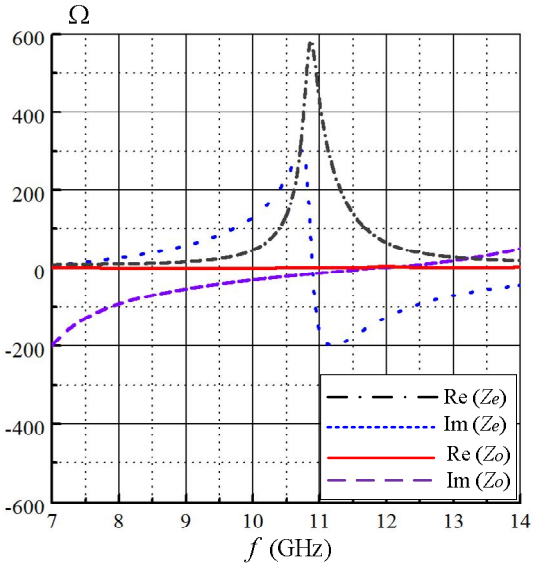

Fig. 6: Imaginary part and real part of even and odd impedance versus frequency.

V. Measured Rresults

One prototype of the proposed coupler is fabricated using TLY031 substrate with ε_r=2.2, h=0.787 mm and loss tangent of 0.009. A photo of the fabricated coupler is shown in Fig. 7.

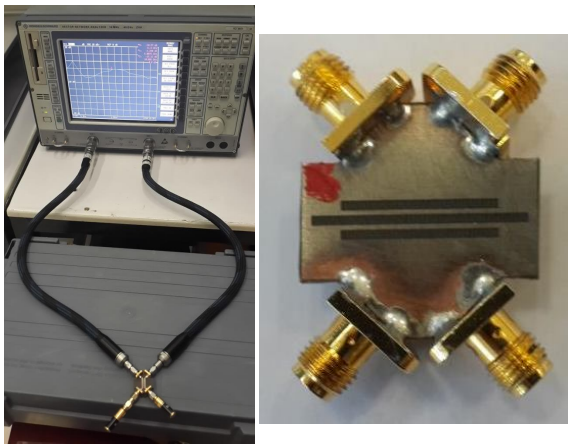

Fig. 7: photo of the fabricated coupler under test bench

The measured results are shown in Fig. 8, including simulation results for comparison. It can be seen that measured coupling is 0.49 dB with 2 dB flatness in the desired bandwidth. Also, measured reflection coefficient is better than 12.45 dB in the pass band. It can be seen that a very good agreement is obtained between measurement and simulation results.

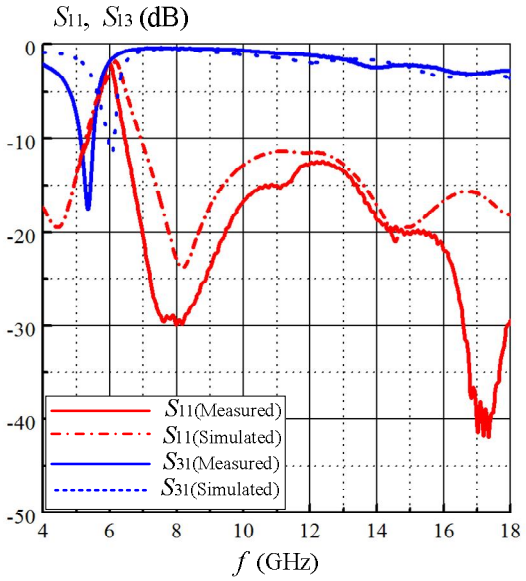

Fig. 8: Measured results

VI. Conclusions

This study presents a wideband backward-wave directional coupler. To design the coupler, neural network is used. The operation of this coupler is similar to CRLH coupler in its bandwidth except in the bandwidth from 10 GHz to 13GHz, which operates like conventional couplers in it. The coupler that was proposed in this chapter has the advantage of high coupling with 1 dB flatness in a very wide bandwidth. This coupler is fabricated. Fabrication results agree well with simulation results.

VII. REFERENCES

[1] L. K. Yeung, K. Wu, "A Dual-Band Coupled Line Balun Filter," *IEEE Transactions on Microwave Theory and Techniques*, vol.55, pp. 2406 - 2411, 2007.

[2] A. M. Qaroot, N. I. Dib, "General Design of N-Way Multi-Frequency Unequal Split Wilkinson Power Divider Using Transmission Line Transformers," *Progress In Electromagnetics Research C*, vol.14, pp. 115 - 129, 2010.

[3] C. Caloz and T. Itoh, "Guided-wave applications" in Electromagnetic metamaterials: *transmission line theory and microwave applications*, 1st ed., Ed. New Jersey: John Wiley & Sons, 2006, pp. 227-249.

[4] J. Lange, "Interdigital stripline quadrature hybrid," *IEEE Trans. Microwave Theory Tech*.,vol. 17, no. 12, pp. 1150–1151, Dec. 1969.

[5] C. Caloz, A. Sanada, and T. Itoh. "A novel composite right/left-handed coupled-line directional coupler with arbitrary coupling level and broad bandwidth," *IEEE Trans. Microwave Theory Tech*.,vol. 52, no. 3, pp. 980–992, March 2004.

[6] Z. S. Tabatabaeian, and M. H. Neshati, "Design Investigation of an X-Band SIW H-Plane Band Pass Filter with Improved Stop Band Using Neural Network Optimization," *Applied Computational Electromagnetics Society*, vol. 30, no. 10, pp. 1083-1088, Oct. 2015.

[7] Fecit R&D Center of Science and Technology Products, Neural Network Theory and Matlab Implementation. Beijing: Publishing House of Electronics Industry, 2005.

[8] M. Hrobak, M. Sterns, E. Seler, M. Schramm, L. P. Schmidt, "Design and construction of an ultrawideband backward wave directional coupler," *IET Microwaves, Antennas & Propagation*, vol. 6, pp. 1048–1055, Oct. 2012.

[9] Y. Ma, H. Zhang, Y. Li, "Novel Symmetrical Coupled-Line Directional Coupler Based on Resonant-Type Composite Right/Left Handed Transmission Lines," *Progress In Electromagnetics Research*, vol. 140, pp. 213-226, 2013.

[10] M. Chudzik, I. Arnedo, A. Lujambio, I. Arregui, F. Teberio, D. Benito, T. Lopetegi and M. A. G. Laso, "Design of EBG microstrip directional coupler with high directivity and coupling," Proceedings of the 42nd European Microwave Conference, pp. 483-486, 2012.

[11] H. Mextorf and R. Knöchel, "The Intrinsic Impedance and Its Application to Backward and Forward Coupled-Line Couplers," *IEEE Transactions on Microwave Theory and Techniques*, vol. 62, pp. 224 - 233, 2014.

[12] R. Islam, G. V. Eleftheriades, "Review of the microstrip/negative-refractive-index transmission-line coupled-line coupler," *IET Microwaves, Antennas & Propagation*, vol. 6, pp. 31– 45, 2012.

[13] C. Liu and W. Menzel, "A microstrip diplexer from metamaterial transmission lines," *IEEE MTT-S InternationalMicrowave Symposium Digest*, 2009, pp. 65-68.

[14] A. Pourzadi, A. R. Attari, M. S. Majedi, "A directivity-enhanced directional coupler using epsilon negative transmission line," *IEEE Trans. Microwave Theory Tech*., vol. 60, no. 11, pp. 3395–3402, Nov. 2012.